International Journal of Nanomedicine

Dovepress
open access to scientific and medical research

Open Access Full Text Article

ORIGINAL RESEARCH

The effects of magnetite (Fe_3O_4) nanoparticles on electroporation-induced inward currents in pituitary tumor (GH_3) cells and in RAW 264.7 macrophages

This article was published in the following Dove Press journal:
International Journal of Nanomedicine
26 March 2012
Number of times this article has been viewed

Yen-Chin Liu[1]
Ping-Ching Wu[2]
Dar-Bin Shieh[2–5]
Sheng-Nan Wu[3,6,7]

[1]Department of Anesthesiology, [2]Institute of Oral Medicine and Department of Stomatology, [3]Department of Physiology, National Cheng Kung University Hospital, College of Medicine, [4]Advanced Optoelectronic Technology Center, [5]Center for Micro/Nano Science and Technology, National Cheng Kung University, [6]Innovation Center for Advanced Medical Device Technology, National Cheng Kung University, [7]Department of Anatomy and Cell Biology, National Cheng Kung University Medical College, Tainan, Taiwan

Correspondence: Sheng-Nan Wu and Dar-Bin Shieh
Institute of Basic Medical Sciences, National Cheng Kung University College of Medicine and Hospital, Tainan 70101, Taiwan
Tel +886 6 2353534 5334 and 5813
Fax +886 6 2362780 and 2359885
Email snwu@mail.ncku.edu.tw; dbshieh@mail.ncku.edu.tw

Aims: Fe_3O_4 nanoparticles (NPs) have been known to provide a distinct image contrast effect for magnetic resonance imaging owing to their super paramagnetic properties on local magnetic fields. However, the possible effects of these NPs on membrane ion currents that concurrently induce local magnetic field perturbation remain unclear.

Methods: We evaluated whether amine surface-modified Fe_3O_4 NPs have any effect on ion currents in pituitary tumor (GH_3) cells via voltage clamp methods.

Results: The addition of Fe_3O_4 NPs decreases the amplitude of membrane electroporation-induced currents (I_{MEP}) with a half-maximal inhibitory concentration at 45 μg/mL. Fe_3O_4 NPs at a concentration of 3 mg/mL produced a biphasic response in the amplitude of I_{MEP}, ie, an initial decrease followed by a sustained increase. A similar effect was also noted in RAW 264.7 macrophages.

Conclusion: The modulation of magnetic electroporation-induced currents by Fe_3O_4 NPs constitutes an important approach for cell tracking under various imaging modalities or facilitated drug delivery.

Keywords: iron oxide, ion current, free radical

Introduction

Studies of nanoscale materials have captured significant scientific and industrial interest in recent years. Magnetite (Fe_3O_4) nanoparticles (NPs) have been extensively exploited as ferrofluids in various industrial applications. They respond to electromagnetic energy by changing surface anisotropy and thus could generate heat in microenvironments for clinical therapeutics. Fe_3O_4 NPs usually present super paramagnetic properties and by altering proton relaxation in the tissue microenvironment are ideal for magnetic resonance contrast enhancement.[1,2] Recent studies have described an aqueous preparation protocol for well-dispersed Fe_3O_4 NPs by coprecipitation of Fe(II) and Fe(III) in the presence of organic acid.[3,4] The derived magnetite NPs present a stable surface amine group without a polymer coating that could nonetheless be well dispersed in the aqueous phase and in tissue fluid.

Magnetic NPs have been reported to stimulate mechanosensitive ion channels.[5] The presence of superparamagnetic nanoparticles could alter the local magnetic field permeability and distribution thereby affecting local currents in the microenvironment. Other types of nanomaterials such as carbon nanotubes have been reported to influence the

amplitude of K^+ currents.[6–8] However, to our knowledge, the mechanisms through which these magnetite NPs can interact with cells, or specifically ion channels, remain unclear.

It is recognized that membrane electroporation (MEP) exerts a considerable increase in the electrical conductivity and permeability of the plasma membrane with the aid of an externally applied electrical field.[9] This maneuver is commonly used for transferring DNA and chemotherapeutic drugs into cells, and was recently applied to cell labeling with Fe_3O_4 NPs.[1,9,10] In GH_3 pituitary tumor cells, we have identified a unique type of membrane hyperpolarization-induced inward current referred to as an MEP-induced current (I_{MEP}), that is sensitive to the inhibition of memantine and $LaCl_3$ and to the stimulation of honokiol, a dimer of allylphenol.[11] Owing to the high conductance of MEP-induced channels, even at low probability of opening, significant currents tend to flow and may thereby alter the electrical behavior of the porated cells.

Therefore, the purpose of this work is to evaluate whether Fe_3O_4 NPs with a mean diameter of 6 nm could exert functional effects on the ion currents in pituitary tumor (GH_3) cells. Interestingly, findings from our study indicate that Fe_3O_4 NPs are effective in decreasing the amplitude of I_{MEP} in a concentration-dependent manner in these cells. Higher concentrations (3 mg/mL) of these particles were also noted to increase I_{MEP} amplitude.

Materials and methods

Drugs and solutions

4,4′-Dithiodipyridine, lipopolysaccharide, single-walled carbon nanotubes (0.7–1.1 nm in diameter), sodium hydroxide, and tetrodotoxin were obtained from Sigma-Aldrich (St, Louis, MO), and 2,2′-azo-bis(2-amidinopropane) dihydrochloride (AAPH) was obtained from Wako Pure Industries (Osaka, Japan). All culture media, fetal calf serum, horse serum, L-glutamine, trypsin/ethylenediaminetetraacetic acid, and penicillin–streptomycin were obtained from Invitrogen (Carlsbad, CA). All other chemicals, including CsCl, $CdCl_2$, $FeCl_2$, $FeCl_3$, $LaCl_3$, and *N*-methyl-D-glucamine$^+$, were commercially available and of reagent grade.

The composition of normal Tyrode's solution is as follows (in mM): NaCl 136.5, KCl 5.4, $CaCl_2$ 1.8, $MgCl_2$ 0.53, glucose 5.5, and 4-(2-hydroxyethyl)-1-piperazineethanesulfonic acid (HEPES)–NaOH buffer 5.5 (pH 7.4). To record I_{MEP} or delayed rectifier K^+ current ($I_{K(DR)}$), the patch pipette was filled with a solution (in mM): K-aspartate 130, KCl 20, KH_2PO_4 1, $MgCl_2$ 1, Na_2 ATP 3, Na_2GTP 0.1, ethylene glycol tetraacetic acid 0.1, and HEPES–KOH buffer 5 (pH 7.2). To measure voltage-gated Ca^{2+} currents, K^+ ions in the pipette solution were replaced with equimolar Cs^+ ions and the pH was adjusted to 7.2 with CsOH. To record *erg*-like K^+ currents ($I_{K(erg)}$), the bath solution was replaced with a high-K^+, Ca^{2+}-free solution (in mM): KCl 130, NaCl 10, $MgCl_2$ 3, glucose 6, and HEPES–KOH buffer 10 (pH 7.4).

Preparation of dispersed, water-soluble Fe_3O_4 NPs

Fe_3O_4 NPs with an average diameter of 6 nm were prepared without a polymer coating as described previously.[3,4] Briefly, a protective agent was added in two stages followed by chemical co-precipitation. The aqueous solutions containing 2 M Fe(II) and 1 M Fe(III) were prepared by dissolving $FeCl_2$ and $FeCl_3$, respectively. To produce Fe_3O_4 NPs, 1 mL Fe(II) and 4 mL Fe(III) aqueous solutions were mixed at room temperature, followed by the addition of 0.5 g organic acid as adherent. Afterward, 0.5 M NaOH was dropwise added into the mixed solution to adjust the pH. The reaction was finished when the pH of the solution reached 11. The precipitates were then collected by a magnet and washed with 50 mL of deionized water three times, followed by addition of another 3 g of organic acid to achieve complete coating of the particle surface with the $-NH_3^+$ group. The excess adherents were removed by rinsing in deionized water. The size of the Fe_3O_4 NPs was determined by analytical scanning transmission electron microscopy (JEOL 3010; JEOL, Tokyo, Japan). The particle concentration was analyzed using an atomic absorption spectrometer (Solaar M6 series; Unicam Audio Visual, Leeds, UK), where iron oxides were treated with nitric or hydrochloride acid until complete dissolution.

Cell preparation

GH_3 pituitary tumor cells, obtained from the Bioresources Collection and Research Center ([BCRC-60015]; Hsinchu, Taiwan), were maintained in Ham's F-12 medium supplemented with 15% horse serum, 2.5% fetal calf serum, and 2 mM L-glutamine in a humidified environment of 5% CO_2.[11,12] The experiments were performed 5 or 6 days after the cells had been cultured (60%–80% confluence). The colorimetric method was used in examining the viable cell densities in microtiter plates with a tetrazolium salt (4-[3-(4-iodophenyl)-2-(4-nitrophenyl)-2H-5-terasolio]-1,3-benzene disulfonate; WST-1) and an enzyme-linked immunosorbent assay reader (Dynatech, Chantilly, VA). In order to investigate cell viability, GH_3 cells were incubated at 37°C for

24 hours in the media containing different concentrations of Fe_3O_4 NPs.

The murine macrophage cell line RAW 264.7 was obtained from the American Type Culture Collection (TIB-71; ATCC, Manassas, VA). Cells were grown in Dulbecco's modified Eagle's medium supplemented with 10% heat-inactivated fetal bovine serum, 100 U/mL penicillin, and 100 µg/mL streptomycin.[13] When cells were challenged with lipopolysaccharide (0.5 mg/mL), they displayed an irregular form with accelerated spreading and formation of pseudopodia.

Electrophysiological measurements

Before each experiment, GH_3 or RAW 264.7 cells were dissociated and an aliquot of cell suspension was transferred to a recording chamber positioned on the stage of an inverted DM-IL microscope (Leica, Wetzlar, Germany). Cells were bathed at room temperature (25°C) in normal Tyrode's solution containing 1.8 mM $CaCl_2$. Patch electrodes were made from Kimax®-51 capillaries (Kimble Glass, Vineland, NJ) using a PP-830 puller (Narishige, Tokyo, Japan), and they had a resistance of 3–5 MΩ when filled with the different pipette solutions described above. Voltage-clamp recordings were made in whole-cell configuration using an RK-400 amplifier (Bio-Logic, Claix, France) or an Axopatch™ 200B amplifier (Molecular Devices, Sunnyvale, CA).[11,12,14] The I_{MEP} was induced as documented previously.[15]

Measurement of superoxide level

A lucigenin-based chemiluminescence assay was used to detect free radical production similar to that used by Chan et al.[16] Equal numbers (about 8×10^4) of GH_3 cells at 80% confluence were isolated with trypsin/ethylenediaminetetraacetic acid and centrifuged, and then supernatant was removed. Subsequently, 1 mL Tyrode's solution (calcium free) was added. The cell pellet was mixed well and was obtained immediately for O_2^- measurement after magnetic separation. Background chemiluminescence in buffer (2 mL) containing lucigenin (5 µM) was measured for 5 minutes. Final variable concentrations of Fe_3O_4 NPs (30 µg/mL and 3 mg/mL) were then added and chemiluminescence was measured for 2.5 minutes at room temperature with the luminometer (Sirius luminometer, Berthold, Bad Wildbad, Germany). O_2^- production was calculated and expressed as the relative ratio to the control.

Data recordings and analyses

The data were stored online in a TravelMate-6253 computer (Acer, Taipei, Taiwan) at 10 kHz through a Digidata-1322A interface (Molecular Devices). The interface device was equipped with a SlimSCSI card (Adaptec, Milpitas, CA) via a PCMCIA slot and controlled by pCLAMP 9.2 (Molecular Devices). The pCLAMP-generated voltage-step profiles were used to determine the current–voltage (*I–V*) relationship for I_{MEP}.

Concentration – response data for Fe_3O_4 NP-induced block of I_{MEP} in GH_3 cells were fitted with a modified form of the Hill equation.[11] That is,

$$y = 1 - \frac{(1-a) \times [C]^{n_H}}{IC_{50}^{n_H} + [C]^{n_H}},$$

where y is the relative amplitude of I_{MEP}; [C] is the concentration of Fe_3O_4 NPs; IC_{50} and n_H are concentrations required for a 50% inhibition and the Hill coefficient, respectively. Maximal inhibition (ie, 1–*a*) of I_{MEP} in the presence of Fe_3O_4 NPs was also estimated. Curve-fitting to data sets was commonly performed with the aid of Excel 2007 (Microsoft, Redmond, WA) or Origin 8.0 (OriginLab Corp, Northampton, MA).

Values are provided as the mean values ± standard error of the mean with the sample sizes (n) indicating the number of cells from which the data were taken. The paired or unpaired Student's *t*-test and one-way analysis of variance with a least significant difference method for multiple comparisons were used for the statistical evaluation of difference among means. A *P* value of less than 0.05 was considered to indicate statistical difference.

Results

Effect of Fe_3O_4 NPs on I_{MEP} in pituitary GH_3 cells

In an initial set of experiments, whole-cell configuration was obtained to investigate the electrical properties of macroscopic I_{MEP} in these cells. Cells were bathed in Ca^{2+}-free Tyrode's solution containing 10 mM CsCl. When the cell was held at –80 mV, a hyperpolarizing pulse from –80 to –200 mV with a duration of 300 msec was applied. Under this voltage profile, I_{MEP} was generated with a waxing-and-waning pattern.[11] As shown in Figure 1B, we noted that when we exposed the cells to Fe_3O_4 NPs, the amplitude of I_{MEP} was progressively diminished. For example, at the level of –200 mV, these NPs at a concentration of 100 µg/mL significantly decreased the I_{MEP} amplitude from 865 ± 42 to 261 ± 33 pA (n = 9). After washout of the nanoparticles, the current amplitude returned to 757 ± 33 pA (n = 6).

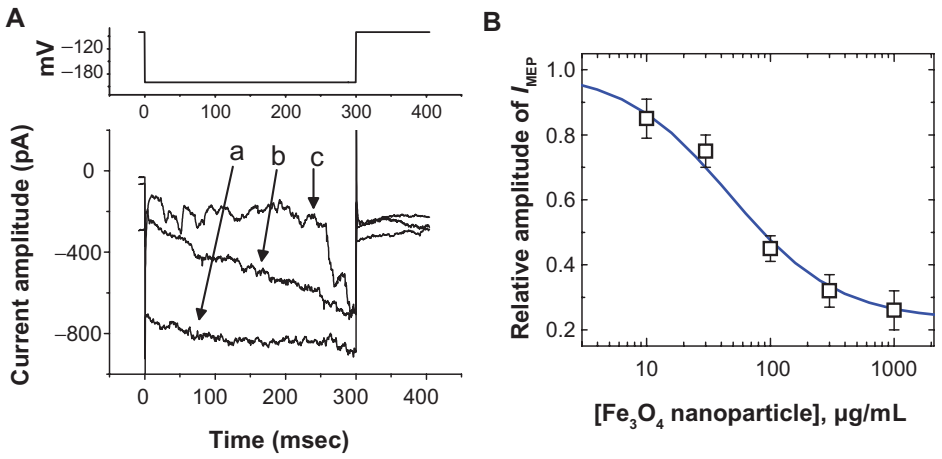

Figure 1 The effect of Fe_3O_4 NPs on I_{MEP} in GH_3 pituitary tumor cells. In these experiments, cells were bathed in Ca^{2+}-free Tyrode's solution containing 10 mM CsCl. The cell was held at –80 mV and hyperpolarizing pulses to –200 mV with a duration of 300 msec at a rate of 0.1 Hz were applied. (**A**) Superimposed current traces obtained in (a) the absence of Fe_3O_4 NPs and (b) the presence of 30 μg/mL Fe_3O_4 NPs and (c) 100 μg/mL Fe_3O_4 NPs. The upper part indicates the voltage protocol used. (**B**) The concentration–response curve for Fe_3O_4 NP-induced inhibition of I_{MEP} in these cells (mean ± standard error of the mean; n = 5–12 for each point). Current amplitudes obtained at the different concentrations (10 μg/mL–1 mg/mL) of Fe_3O_4 NPs were measured at the end of hyperpolarizing pulses (ie, –200 mV). The smooth blue line represents the best fit to the Hill equation as described under Materials and methods.

Note: The IC_{50} value, maximally inhibited percentage of I_{MEP}, and Hill coefficient for NP-induced inhibition of I_{MEP} were calculated to be 45 μg/mL, 23%, and 1.1, respectively.

Abbreviation: Fe_3O_4 NPs, magnetite nanoparticles.

The relationship between the concentration of Fe_3O_4 NPs and the relative amplitude of I_{MEP} was analyzed (Figure 1B). The half-maximal concentration required for the inhibitory effect of Fe_3O_4 NPs was calculated to be 45 μg/mL. Therefore, results from these observations reflect that Fe_3O_4 NPs have an inhibitory effect on I_{MEP} in GH_3 cells.

To characterize the inhibitory effect of Fe_3O_4 NPs on I_{MEP}, we studied whether the nanoparticles could alter the I_{MEP} measured at the different levels of membrane potentials in these cells. Figure 2 shows the *I–V* relations obtained in the absence and presence of Fe_3O_4 NPs. The threshold for elicitation of these inward currents was around –70 mV and current magnitude was noted to become larger with greater hyperpolarization. The results showed that cell exposure to Fe_3O_4 NPs (100 μg/mL) presents a significant decrease in the slope of the linear fit of I_{MEP} amplitudes to voltage between –100 and –200 mV from 10.7 ± 1.1 to 3.6 ± 0.6 nS (n = 9). However, the threshold potential required for elicitation of I_{MEP} did not show Fe_3O_4 NP dependence.

Dual effect of Fe_3O_4 NPs on the amplitude of I_{MEP} in GH_3 cells

We also discovered that when the cells were exposed to high concentrations of Fe_3O_4 NPs (3 mg/mL), a biphasic response in the I_{MEP} amplitude could be recorded, ie, an initial decrease followed by a persistent elevation. Figure 3 illustrates the dual effect of Fe_3O_4 NPs (3 mg/mL) on I_{MEP} in cells bathed in Ca^2 -free Tyrode's solution containing 10 mM CsCl. When the cell was hyperpolarized from –80 to –200 mV, 1 minute after the addition of Fe_3O_4 NPs (3 mg/mL), the amplitude of I_{MEP} was significantly decreased to 685 ± 45 pA from a control value of 1645 ± 115 pA (n = 6). However, 3 minutes after the addition of 3 mg/mL Fe_3O_4 NPs to the solution, the amplitude of I_{MEP} measured at the same level (ie, –200 mV) was found to return to 1382 ± 595 pA (n = 6). Moreover, when

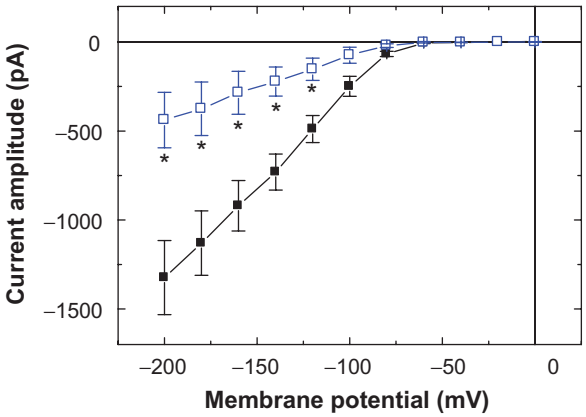

Figure 2 Effects of Fe_3O_4 NPs on *I–V* relation of I_{MEP} in GH_3 cells. In these experiments, cells were bathed in Ca^{2+}-free Tyrode's solution containing 10 mM CsCl, and I_{MEP} was elicited from –50 mV to different potentials ranging from –200 to 0 mV with 20 mV increments. The data (mean ± standard error of the mean; n = 8–11) were obtained in the absence (■) and presence (□) of Fe_3O_4 NPs (100 μg/mL). Notably, addition of the NPs reduced the slope of I_{MEP} at the voltage ranging between –100 and –200 mV, although no change in the threshold potential of this current was observed.

Note: *Significantly different from controls measured at each voltage.

Abbreviation: Fe_3O_4 NPs, magnetite nanoparticles.

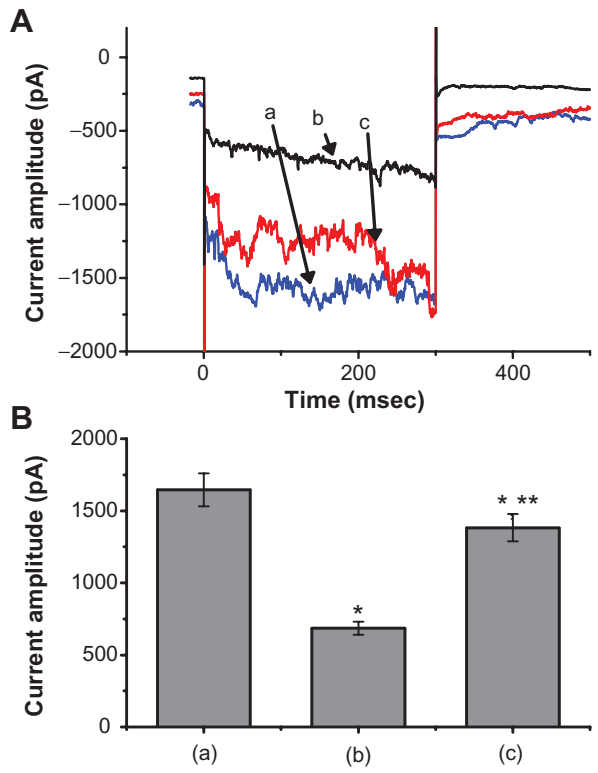

Figure 3 The dual effect of Fe_3O_4 NPs on I_{MEP} in GH_3 cells. In these experiments, cells were bathed in Ca^{2+}-free Tyrode's solution containing 10 mM CsCl. The cell was held at −80 mV and hyperpolarizing steps to −200 mV with a duration of 300 msec at a rate of 0.1 Hz were then delivered. (**A**) Superimposed current traces obtained (a) in the absence of Fe_3O_4 NPs, (b) 1 minute, and (c) 3 minutes after the addition of NPs (3 mg/mL). (**B**) Bar graph showing summary of the effect of 3 mg/mL Fe_3O_4 NPs on I_{MEP} in GH_3 cells (mean ± standard error of the mean; n = 6 for each bar). Bar (a) is the control, and bars (b) and (c) were obtained 1 and 3 minutes after the addition of Fe_3O_4 NPs (3 mg/mL), respectively.
Notes: *Significantly different from control. **Significantly different from those obtained 1 minute after the addition of NPs.
Abbreviation: Fe_3O_4 NPs, magnetite nanoparticles.

cells were pretreated with AAPH (30 μM), the stimulatory effect of the NPs was eliminated. AAPH is known to be a water-soluble initiator of peroxyl radicals.[17] NP-stimulated increase of I_{MEP} is thus likely to be associated with an increase in reactive oxygen species.

Electric properties of MEP-induced channels in the absence and presence of Fe_3O_4 NPs

The effect of Fe_3O_4 NPs on the activity of MEP-induced channels was further investigated. In these experiments, cells were bathed in Ca^2 -free Tyrode's solution containing 10 mM CsCl and 1 mM $LaCl_3$. A ramp pulse from −200 to +100 mV with 1.5 seconds at a rate of 0.05 Hz was applied to the cells. In the control group, the opening events of MEP-elicited channels at the hyperpolarizing potentials were clearly observed, while there was a pronounced outward current elicited by such a long-lasting ramp pulse. Moreover, as shown in Figure 4, when cells were exposed to Fe_3O_4 NPs (100 μg/mL), there was a progressive decrease in the activity of MEP-induced channels, which occurred at the level of hyperpolarizing potentials ranging between −80 and −200 mV. The single-channel amplitude at −150 mV in the absence and presence of Fe_3O_4 NPs (100 μg/mL) was calculated to be 78 ± 9 pA (n = 9) and 76 ± 9 pA (n = 7), respectively. Through such a long-lasting voltage ramp pulse, a fit of the data using a linear *I–V* relationship obtained in the control yielded the single-channel conductance and reversal potential of 0.54 ± 0.08 nS and −27.2 ± 0.9 mV (n = 7). During cell exposure to Fe_3O_4 NPs, the values for these channels were not altered significantly. Therefore, it is clear from these results that the addition of Fe_3O_4 NPs did not modify the single-channel conductance of MEP-elicited channels induced by long-lasting ramp pulses, although it could increase the probability of channel openings.

No effect of Fe_3O_4 NPs on delayed rectifier K^+ current ($I_{K(DR)}$) in GH_3 cells

Carbon nanotubes have been recently described to influence different types of K currents in pheochromocytoma PC12 cells.[7] We further examined whether magnetite NPs could exert specific effects on $I_{K(DR)}$ in GH_3 cells by direct interaction with the channel or local effects on the regional electromagnetic fields. These experiments were conducted in cells bathed in Ca^{2+}-free Tyrode's solution containing 1 μM tetrodotoxin and 0.5 mM $CdCl_2$, and the recording pipette was filled with K^+-containing solution. Tetrodotoxin was used to block Na^+ currents, while $CdCl_2$ could inhibit voltage-gated Ca^{2+} currents. Figure 5 depicts superimposed original traces of $I_{K(DR)}$ obtained in the absence and presence of 100 μg/mL Fe_3O_4 NPs. For example, when the cells were depolarized from −50 to +50 mV, Fe_3O_4 NPs (100 mg/mL) caused no significant effect on the amplitude of $I_{K(DR)}$ measured at the end of the depolarizing pulse (544 ± 32 pA [control] versus 540 ± 29 pA [Fe_3O_4 NPs]; n = 6). The results indicated that unlike I_{MEP} described above, $I_{K(DR)}$ elicited by membrane depolarization remained unaltered in the presence of Fe_3O_4 NPs.

Inability of Fe_3O_4 NPs to block *erg*-like K^+ current ($I_{K(erg)}$) in GH_3 cells

We further investigated the possible effect of the synthesized NPs on $I_{K(erg)}$ enriched in GH_3 cells.[18,19] As shown in Figure 6, addition of the nanoparticles did not cause any effect on $I_{K(erg)}$ in these cells. The peak amplitude of $I_{K(erg)}$ elicited by

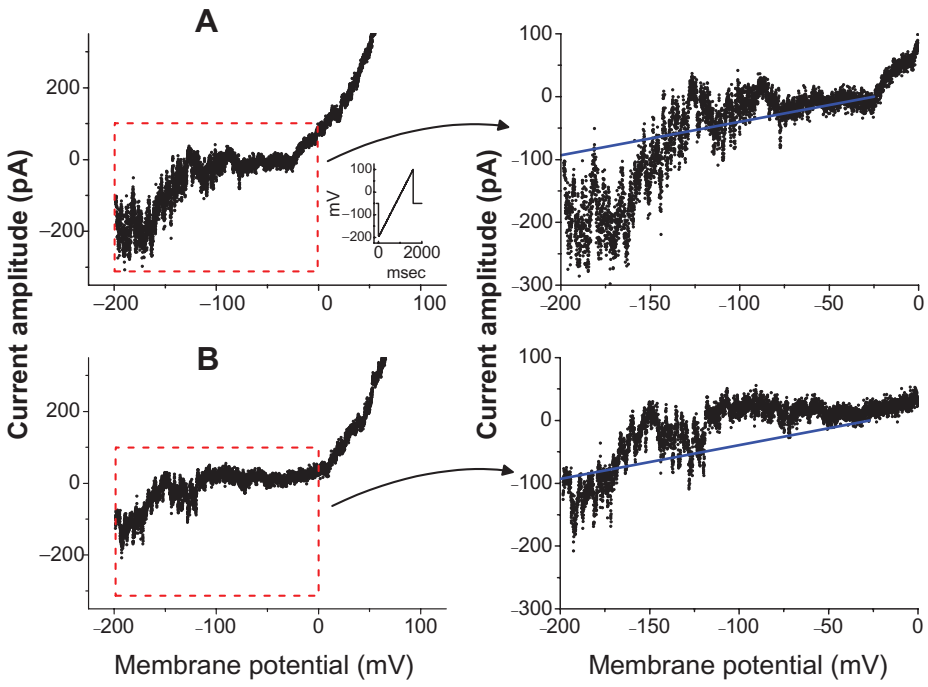

Figure 4 Activity of membrane electroporation-induced channels in the absence (**A**) and presence (**B**) of Fe_3O_4 NPs in GH_3 cells. In these experiments, cells were bathed in Ca^{2+}-free Tyrode's solution containing 10 mM CsCl and 1 mM $LaCl_3$. Single-channel events were elicited by long-lasting ramp pulse ranging between –200 and +100 mV with a duration of 1.5 seconds at a rate of 0.05 Hz. Downward deflections indicate the opening events of the channel. The inset in (**A**) indicates the voltage protocol examined. The right-hand graph in (**A**) and (**B**) represents an amplified current trace corresponding to that appearing in the red dashed box in the left-hand graph.

Notes: The straight blue line shown on the right side illustrates a linear *I–V* relation of membrane electroporation-elicited channels in (**A**) control and (**B**) during exposure to Fe_3O_4 NPs (100 μg/mL). Notably, no change in single-channel conductance was demonstrated in the presence of Fe_3O_4 NPs, although it decreased the probability of channel openings.

Abbreviation: Fe_3O_4 NPs, magnetite nanoparticle.

membrane hyperpolarization from –10 to –90 mV was not noted to differ significantly between the absence and presence of 100 μg/mL Fe_3O_4 NPs (1485 ± 122 pA [control] versus 1481 ± 95 pA [Fe_3O_4 NPs]; n = 7). However, similar to previous reports,[6,19] methadone (10 μM) and single-walled carbon nanotubes (30 μg/mL) could significantly reduce the amplitude of $I_{K(erg)}$ by 44% and 29%, respectively.

Effect of Fe_3O_4 NPs on I_{MEP} in RAW 264.7 cells

Previous studies of the magnetic resonance imaging of lymph node have demonstrated that Fe_3O_4 NPs can be effectively taken up by macrophages in the reticuloendothelial system.[2,20–24] Therefore, we examined the effect of Fe_3O_4 NPs on the I_{MEP} recorded from RAW 264.7 macrophages. RAW 264.7 is a macrophage-like, Abelson leukemia virus-transformed cell line known to possess the characteristics of macrophages.[13] As shown in Figure 7, the properties of I_{MEP} in RAW 264.7 cells were characterized with the same voltage profile employed in GH_3 cells. During whole-cell recordings, when membrane hyperpolarizations from –80 to –200 mV were applied to the cells, an irregular and transient inward current was elicited. In response to membrane hyperpolarization these inward currents comprised multiple small currents occurring asynchronously. When the bathing solution was replaced by $NMDA^+$ solution, this current could still be induced, although the magnitude of inward currents was diminished. Unlike mechanosensitive ion currents,[5,25] this type of inward current noted in RAW 264.7 cells is thus referred to as an I_{MEP}.[11] Interestingly, when these cells were exposed to Fe_3O_4 NPs, the I_{MEP} amplitude was progressively diminished (Figure 7). For example, the addition of Fe_3O_4 NPs (100 μg/mL) significantly decreased the I_{MEP} amplitude at –200 mV from 924 ± 55 to 403 ± 19 pA (n = 7). The results were consistent with the observations made in GH_3 cells. The Fe_3O_4 NPs were capable of producing an inhibitory action on hyperpolarization-induced I_{MEP} in RAW 264.7 macrophages.

Effect of Fe_3O_4 NPs on the production of superoxide in GH_3 cells

Superoxide production is shown in Figure 8 and demonstrated that Fe_3O_4 NPs produced a biphasic pattern in the

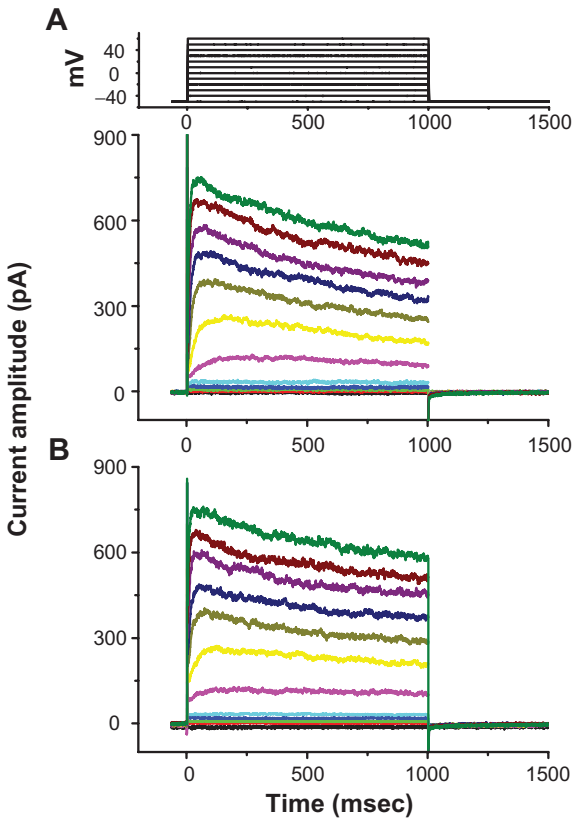

Figure 5 Lack of effect of Fe_3O_4 NPs on delayed rectifier K^+ current ($I_{K(DR)}$) in GH_3 cells. Cells, immersed in Ca^{2+}-free Tyrode's solution containing 1 μM tetrodotoxin and 0.5 mM $CdCl_2$, were held at –50 mV and depolarizing pulses ranging from –50 to +60 mV in 10 mV increments with a duration of 1 second were applied. Superimposed current traces shown in (**A**) are control, and those in (**B**) were recorded 2 minutes after the addition of 100 μg/mL Fe_3O_4 NPs. No discernible change in $I_{K(DR)}$ kinetics and amplitude was demonstrated when cells were exposed to Fe_3O_4 NPs.
Note: The uppermost part indicates the voltage protocol used.
Abbreviation: Fe_3O_4 NPs, magnetite nanoparticles.

superoxide generation to 0.38 ± 0.26 (100 μg/mL) and 13.71 ± 0.47 (3 mg/mL), respectively ($P = 0.04$, $P < 0.01$, respectively) when compared to the control (1.00 ± 0.14). Interestingly, Fe_3O_4 NPs also increase the reactive oxygen species production to 8.15 ± 1.78 (3 mg/mL; $P = 0.01$,) but not in the low-dose group (0.95 ± 0.49 [100 μg/mL]).

Discussion

In this study, aqueous dispersive Fe_3O_4 NPs were found to exert both excitatory and inhibitory effects on I_{MEP} in pituitary GH_3 cells. Lower concentrations of Fe_3O_4 NPs suppressed the amplitude of I_{MEP}, while higher concentrations of these NPs could increase I_{MEP}. However, the stimulation of I_{MEP} caused by Fe_3O_4 NPs was abolished in cells pretreated with AAPH (30 μM). AAPH is an azo compound that could generate free radicals.[17] Superoxide production was significantly increased in the presence of Fe_3O_4 NPs. Thus it is conceivable that the stimulatory effect on I_{MEP} observed in GH_3 cells induced by the magnetite nanoparticles might be related to the production of free radicals.

Surface functionalization of nanomaterials is a key factor in their biological and physicochemical properties.[26] Ferumoxtran-10-enhanced magnetic resonance imaging has also been used for improved detection of lymph node metastases in patients with advanced cancer.[2,22,23] The labeling of cells with magnetoelectroporation was described to cause loss of cell viability.[27] In our study, we provided a rationale for this observation as magnetite nanoparticles per se significantly affect the required electric profile for this activity. Therefore, the optimal condition for best poration efficiency and cell viability should be carefully adjusted. It has also been reported that manganese oxide NPs at higher concentrations could be toxic to cancer cells, including glioma cells, Caco-2 cells, and MCF-7 breast cancer cells.[1,28] In our study, Fe_3O_4 NPs at the concentration of 3 mg/mL produced superoxide and stimulated the amplitude of I_{MEP}, consistent with previous reports.[29]

Previous Fourier transform infrared spectroscopy and zeta potential measurements showed the cationic surface of our magnetite NPs to be mostly decorated with $–NH_3^+$. The positively charged surface enabled the nanoparticles to be adsorbed onto the negatively charged cell membrane and to react with I_{MEP} via an electrostatic interaction and local electromagnetic field perturbation. Furthermore, the synthesized Fe_3O_4 NPs were found to self-assemble into a rod-like configuration in aqueous solution.[3] It is possible that Fe_3O_4 NPs may interact with the electropores with a surface charge that produced an electrostatic attraction for binding to the magnetite nanoparticles. The steric hindrance effect by the nanoparticles may block the transportation of cations through the pores and thereby lead to a decrease in I_{MEP} amplitude. The addition of these NPs does not affect $I_{K(DR)}$ or $I_{K(erg)}$. Whether the mechanisms through which NP-induced inhibition of I_{MEP} occurs are linked to the conformational transformation of NPs from spheres to rod shape, and to what extent the local perturbation in the electromagnetic field property affects I_{MEP} remain to be further delineated.

Based on the electrical properties of both I_{MEP} and MEP-induced channels,[11] NP-induced effects on I_{MEP} in GH_3 and RAW 264.7 cells are unlikely to be linked to its action on mechanosensitive ion channels.[5,25] In this study, we show that Fe_3O_4 NP-mediated decrease of I_{MEP} in GH_3 cells is not derived from the decrease in single-channel amplitude of MEP-elicited channels because neither the presence nor the absence of the NPs significantly affected single-channel conductance in these channels. We speculate that the Fe_3O_4

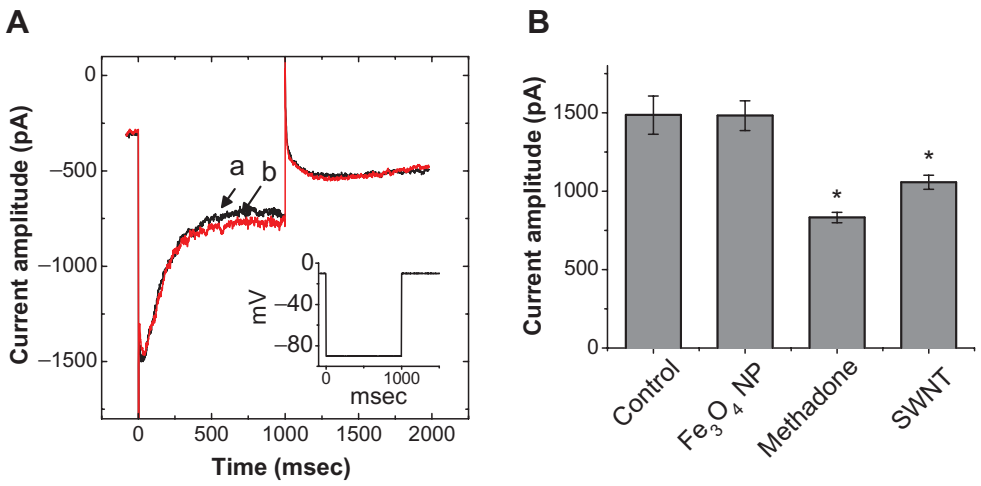

Figure 6 No effect of Fe_3O_4 NPs on $I_{K(erg)}$ in GH_3 cells. In these experiments, cells were bathed in a high-K^+, Ca^{2+}-free solution. Each cell was held at −10 mV and a 1-second long hyperpolarizing pulse from −10 to −90 mV at a rate of 0.01 Hz was applied. (**A**) Superimposed $I_{K(erg)}$ obtained in the absence (a) and presence (b) of 100 μg/mL Fe_3O_4 NPs. The inset indicates the voltage protocol used. (**B**) Bar graph showing summary of the effects of Fe_3O_4 NPs (100 μg/mL), methadone (10 μM), and single-walled nanotubes (30 μg/mL) on $I_{K(erg)}$ (mean ± standard error of the mean; n = 5–7 for each bar). The peak amplitude of $I_{K(erg)}$ in response to membrane hyperpolarization from −10 to −90 mV was measured in each cell. I_{MEP} amplitudes obtained in different concentrations of NPs were measured at −200 mV.
Note: *Significantly different from control.
Abbreviations: Fe_3O_4 NPs, magnetite nanoparticles; SWNT, single-walled nanotubes.

NP-mediated inhibition of I_{MEP} described here could be attributed to the reduced probability of channel openings, the decrease in the number of MEP-elicited pores, or both.

The cytotoxicity of Fe_3O_4 had been previously investigated in our groups before. It demonstrated almost no cytotoxicity in the cell model.[3] Application of a local electrical field could induce transient perturbation of membrane lipids and led to the generation of electroporated channels lined by negatively charged phospholipids. During the MEP process, Fe_3O_4 NPs could be transported into the cells via an accelerated process through charge–charge interaction between the lipid bilayer and the positively charged nanoparticles during the transient channel opening and recovery. Consequently, access of cations to the

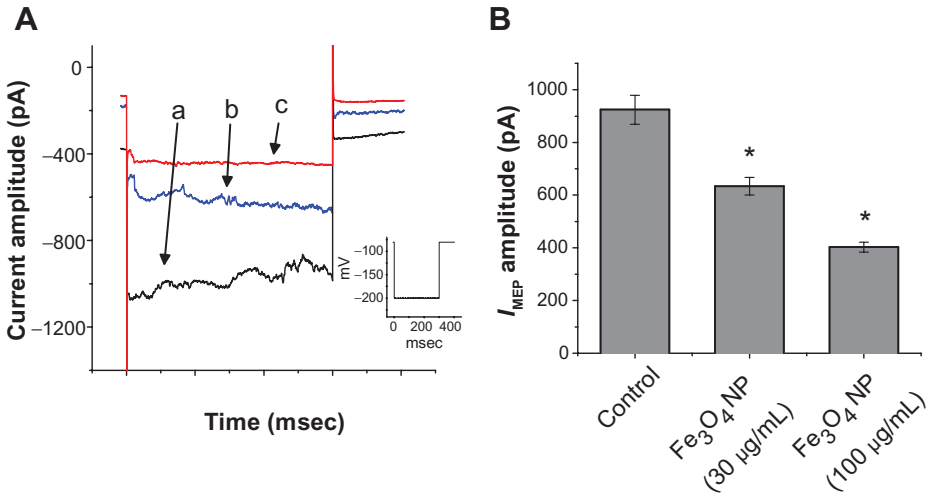

Figure 7 Effect of Fe_3O_4 NPs on I_{MEP} recorded from RAW 264.7 macrophages. The experiments were conducted in cells bathed in Ca^{2+}-free Tyrode's solution. (**A**) Original traces of I_{MEP} obtained in the absence and presence of Fe_3O_4 NPs. The current trace labeled (a) is control, and those labeled (b) and (c) were obtained in the presence of 30 μg/mL and 100 μg/mL Fe_3O_4 NPs, respectively. The inset indicates the voltage protocol used. (**B**) Bar graph showing summary of the effects of Fe_3O_4 NPs (30 μg/mL and 100 μg/mL) on I_{MEP} recorded from RAW 264.7 macrophages (mean ± standard error of the mean; n = 6–10 for each bar).
Note: *Significantly different from control.
Abbreviation: Fe_3O_4 NPs, magnetite nanoparticles.

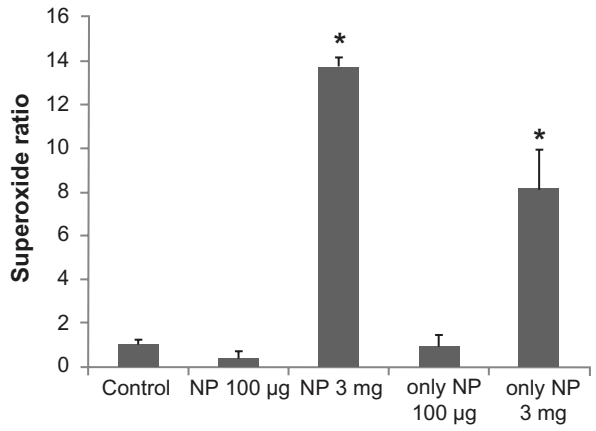

Figure 8 The effect of Fe_3O_4 NPs on superoxide production in GH_3 cells. The experiments were conducted in cells bathed in Ca^{2+}-free Tyrode's solution. Bar graph showing summary of the effects of Fe_3O_4 NPs (100 µg/mL and 3 mg/mL) with or without GH_3 cells (mean ± standard error of the mean; n = 4–5 for each bar).
Note: *Significantly different from control.
Abbreviation: Fe_3O_4 NPs, magnetite nanoparticles.

pore induced by membrane hyperpolarization would be hindered. In our study, the inhibitory effect of Fe_3O_4 NPs on I_{MEP} with a half-maximal inhibitory concentration (IC_{50}) value of 46 µM could derive from the direct binding of the nanoparticles to the pores of the MEP-induced channels. We also observed the inhibitory effect of Fe_3O_4 NPs on I_{MEP} in RAW 264.7 macrophages. Thus the magnetite NPs might also preferentially accumulate around the sites where MEP-elicited channels occurred. Additionally, how the surface functionalization of the magnetite NPs would affect the activity of MEP-elicited channels remains to be explored systematically.

Acknowledgments

This work was partially aided by a grant from the National Science Council (NSC-98-2320-B-006-MY3), and National Cheng Kung University Hospital (NCKUH-10104020), Taiwan, through a contract awarded to SN Wu and DB Shieh. The authors would like to thank Pei-Yu Wu for providing RAW 264.7 cells, Tai-I Hsu for performing parts of the electrophysiological experiments, and Hsien-Ching Huang and Chia-Chen Yeh for their helpful assistance.

Disclosure

The authors report no conflicts of interest in this work.

References

1. Gilad AA, Walczak P, McMahon MT, et al. MR tracking of transplanted cells with "positive contrast" using manganese oxide nanoparticles. *Magn Reson Med*. 2008;60(1):1–7.
2. Oghabian MA, Gharehaghaji N, Amirmohseni S, Khoei S, Guiti M. Detection sensitivity of lymph nodes of various sizes using USPIO nanoparticles in magnetic resonance imaging. *Nanomedicine*. 2010;6(3):496–499.
3. Shieh DB, Cheng FY, Su CH, et al. Aqueous dispersions of magnetite nanoparticles with NH3+ surfaces for magnetic manipulations of biomolecules and MRI contrast agents. *Biomaterials*. 2005;26(34):7183–7191.
4. Wu PC, Su CH, Cheng FY, et al. Modularly assembled magnetite nanoparticles enhance in vivo targeting for magnetic resonance cancer imaging. *Bioconjug Chem*. 2008;19(10):1972–1979.
5. Hughes S, El Haj AJ, Dobson J. Magnetic micro- and nanoparticle mediated activation of mechanosensitive ion channels. *Med Eng Phys*. 2005;27(9):754–762.
6. Park KH, Chhowalla M, Iqbal Z, Sesti F. Single-walled carbon nanotubes are a new class of ion channel blockers. *J Biol Chem*. 2003;278(50):50212–50216.
7. Xu H, Bai J, Meng J, Hao W, Cao JM. Multi-walled carbon nanotubes suppress potassium channel activities in PC12 cells. *Nanotechnology*. 2009;20(28):285102.
8. Liu L, Chen B, Teng F, et al. Effect of Fe(3)O(4)-magnetic nanoparticles on acute exercise enhanced KCNQ(1) expression in mouse cardiac muscle. *Int J Nanomedicine*. 2010;5:109–116.
9. Wang M, Orwar O, Olofsson J, Weber SG. Single-cell electroporation. *Anal Bioanal Chem*. 2010;397(8):3235–3248.
10. Walczak P, Kedziorek DA, Gilad AA, Lin S, Bulte JW. Instant MR labeling of stem cells using magnetoelectroporation. *Magn Reson Med*. 2005;54(4):769–774.
11. Wu SN, Huang HC, Yeh CC, Yang WH, Lo YC. Inhibitory effect of memantine, an NMDA-receptor antagonist, on electroporation-induced inward currents in pituitary GH3 cells. *Biochem Biophys Res Commun*. 2011;405(3):508–513.
12. Liu YC, Wang YJ, Wu PY, Wu SN. Tramadol-induced block of hyperpolarization-activated cation current in rat pituitary lactotrophs. *Naunyn Schmiedebergs Arch Pharmacol*. 2009;379(2):127–135.
13. Wu SN, Wu PY, Tsai ML. Characterization of TRPM8-like channels activated by the cooling agent icilin in the macrophage cell line RAW 264.7. *J Membr Biol*. 2011;241(1):11–20.
14. Shieh DB, Yang SR, Shi XY, Wu YN, Wu SN. Properties of BK(Ca) channels in oral keratinocytes. *J Dent Res*. 2005;84(5):468–473.
15. Wu SN, Huang HC, Yeh CC, Yang WH, Lo YC. Inhibitory effect of memantine, an NMDA-receptor antagonist, on electoporation-induced inward currents in pituitary GH3 cells. *Biochem Biophys Res Commun*. 2011;405(3):508–513.
16. Chan SH, Tai MH, Li CY, Chan JY. Reduction in molecular synthesis or enzyme activity of superoxide dismutases and catalase contributes to oxidative stress and neurogenic hypertension in spontaneously hypertensive rats. *Free Radic Biol Med*. 2006;40(11):2028–2039.
17. Huang MH, Wu SN, Shen AY. Stimulatory actions of thymol, a natural product, on Ca(2+)-activated K(+) current in pituitary GH(3) cells. *Planta Med*. 2005;71(12):1093–1098.
18. Liu YC, Wu SN. Block of erg current by linoleoylamide, a sleep-inducing agent, in pituitary GH3 cells. *Eur J Pharmacol*. 2003;458(1–2):37–47.
19. Huang MH, Shen AY, Wang TS, et al. Inhibitory action of methadone and its metabolites on erg-mediated K+ current in GH pituitary tumor cells. *Toxicology*.2011;280(1–2):1–9.
20. Weissleder R, Elizondo G, Wittenberg J, Lee AS, Josephson L, Brady TJ. Ultrasmall superparamagnetic iron oxide: an intravenous contrast agent for assessing lymph nodes with MR imaging. *Radiology*. 1990;175(2):494–498.
21. Nishimura H, Tanigawa N, Hiramatsu M, Tatsumi Y, Matsuki M, Narabayashi I. Preoperative esophageal cancer staging: magnetic resonance imaging of lymph node with ferumoxtran-10, an ultrasmall superparamagnetic iron oxide. *J Am Coll Surg*. 2006;202(4):604–611.

22. Koh DM, George C, Temple L, et al. Diagnostic accuracy of nodal enhancement pattern of rectal cancer at MRI enhanced with ultrasmall superparamagnetic iron oxide: findings in pathologically matched mesorectal lymph nodes. *AJR Am J Roentgenol*. 2010;194(6): W505–W513.
23. Saokar A, Gee MS, Islam T, Mueller PR, Harisinghani MG. Appearance of primary lymphoid malignancies on lymphotropic nanoparticle-enhanced magnetic resonance imaging using ferumoxtran-10. *Clin Imaging*. 2010;34(6):448–452.
24. Sofue K, Tsurusaki M, Miyake M, Sakurada A, Arai Y, Sugimura K. Detection of hepatic metastases by superparamagnetic iron oxide-enhanced MR imaging: prospective comparison between 1.5-T and 3.0-T images in the same patients. *Eur Radiol*. 2010;20(9):2265–2273.
25. Wu SN, Lin PH, Hsieh KS, Liu YC, Chiang HT. Behavior of nonselective cation channels and large-conductance Ca2+-activated K+ channels induced by dynamic changes in membrane stretch in cultured smooth muscle cells of human coronary artery. *J Cardiovasc Electrophysiol*. 2003;14(1):44–51.
26. Bouffier L, Yiu HH, Rosseinsky MJ. Chemical grafting of a DNA intercalator probe onto functional iron oxide nanoparticles: a physico-chemical study. *Langmuir*. 2011;27(10):6185–6192.
27. Daldrup-Link HE, Meier R, Rudelius M, et al. In vivo tracking of genetically engineered, anti-HER2/neu directed natural killer cells to HER2/neu positive mammary tumors with magnetic resonance imaging. *Eur Radiol*. 2005;15(1):4–13.
28. Rodriguez-Luccioni HL, Latorre-Esteves M, Mendez-Vega J, et al. Enhanced reduction in cell viability by hyperthermia induced by magnetic nanoparticles. *Int J Nanomedicine*. 2011;6:373–380.
29. Zhu MT, Wang Y, Feng WY, et al. Oxidative stress and apoptosis induced by iron oxide nanoparticles in cultured human umbilical endothelial cells. *J Nanosci Nanotechnol*. 2010;10(12):8584–8590.